

Garlic Extract as an Environmentally Corrosion Inhibitor of API X60 Carbon Steel and 316L Stainless Steel in Sulphuric Acid

S. Belkaid^{1*}, S. Hamdani² and D. Mansour³

¹Department of Chemistry, Faculty of Sciences, M'Hamed Bougara University, Avenue de l'Indépendance, Boumerdes, Algeria

²Electrical and Industrial Systems Laboratory, University of Science and Technology Houari Boumediene, P. O. Box 32, El Alia, Bab Ezzouar, Algeria

³Corrosion laboratory, Laboratories-Sonatrach Division, Avenue 1^{er} novembre, Boumerdes, Algeria

*Corresponding author: s.belkaid@univ-boumerdes.dz

Received 30/05/2020; accepted 05/10/2021
<https://doi.org/10.4152/pea.2022400403>

Abstract

The high toxicity of industrial metal corrosion inhibitors raises various environmental and health problems. Thus, the study of metals and alloys corrosion inhibition, in acidic media, by eco-compatible organic compounds, has become a very attractive research field. In this paper, garlic (*Allium Sativum*) extract inhibition efficiency (IE) against API X60 carbon steel (CS) and 316L stainless steel (SS) corrosion, in a 1 M sulphuric acid (H₂SO₄) solution, has been investigated using electrochemical techniques, including potentiodynamic polarization (PPD) and electrochemical impedance spectroscopy (EIS). The experimental results showed the remarkable corrosion inhibitive performance of garlic extract (GE). The corrosion IE, which depends on the inhibitor concentration, increased up to 90%, for SS, and 67% for CS, as shown from the PPD tests. EIS analysis showed that the corrosion resistance (CRST) was increased in the medium with GE, indicating the properties improvement of the passive films formed on the steels surfaces.

Keywords: corrosion, steel, H₂SO₄, green inhibitor and GE.

Introduction

Metals corrosion phenomena are responsible for numerous losses, mainly in the industrial field. Corrosion prevention processes include several measures, such as cathodic protection, surface treatments, or the control of aggressive environments by inhibitors, of which desired performances are assessed in terms of metallic and environmental protection.

Due to the high toxicity of industrial corrosion inhibitors, such as chromate, phosphate and some organic compounds, which are related to various environmental and health problems, their use has been restricted. This is the main reason why many studies have been made to develop the so-called green inhibitors, from plant extracts, essential oils and purified compounds [1-3]. Some

works report that plants have a complex composition and various organic and inorganic compounds that can inhibit steel corrosion [4-6].

The organic compounds include phenols, alcohols, ketones, steroids, saponins, aldehydes, proteins, etc. [7-9]. They form a protective hydrophobic film through the chemisorption mechanism of molecules onto the metal surface, which provides a barrier against its dissolution in the electrolyte [10, 11]. This phenomenon is due to the presence of polar functional groups with oxygen, nitrogen or sulphur atoms, heterocyclic compounds and pi-electrons, which are the reaction centre for the onset of the adsorption process, by transferring electrons to the metal, and forming a covalent coordinate bond [1, 12].

Garlic is known as one of the richest plants, since it contains high concentrations of organic sulphur (S) compounds, such as allin, allicin, ajoene, allylpropyl, diallyl, trisulphide, sallylcysteine and vinylthiines. Furthermore, it contains amino acids and their glycosides, several minerals, such as selenium (Se), zinc (Zn), iron (Fe) and magnesium (Mg), and enzymes, such as allinase, peroxidase and myrosinase [13-15]. The composition of one garlic species may vary according to geographical location, climatic conditions, harvest period, the part of the plant, etc.

Allicin, the major garlic compound, has revealed antibacterial, antiviral and antiparasitic effects [16, 17]. It has been claimed that it can help to prevent cancer risk and platelet aggregation, reduce cholesterol and triglyceride levels, and decrease blood pressure [17, 18]. The use of Allicin as a corrosion inhibitor has been tested for aluminum in acidic [13] and basic [20] media.

Barreto et al. [21] reported that the peeled GE has effectively inhibited 1020 CS corrosion in 0.5 M H₂SO₄. These results become even more relevant for industrial applications, once they have been generalized on other steels and environments.

H₂SO₄ is one of the most widely used inorganic acids for metallic pickling and descaling in industrial processes, as well as in the leaching of many metals from their ores. However, it is highly corrosive for metals and their alloys, especially for CS, which is widely used as an engineering material [19].

Contrary to this class of steel, the presence of a minimum of 10.5% chromium in 316L SS gives it the CRST property. 316L is the common austenitic grade that has a wide range of medical, food and industrial uses. Generalized corrosion occurs when 316L is in contact with an acidic medium, and localized corrosion mostly takes place when it is in a neutral chloride environment.

The aim of the present work was to study an eco-compatible corrosion inhibitor obtained from natural and available raw materials. The effect of GE, at different concentrations, on the behaviour of API X60 carbon and 316L SS in a 1 M H₂SO₄ solution, has been studied by means of different electrochemical techniques, such as PPD and EIS.

Materials and methods

Material and solutions preparation

API X60 and 316L steels have been used throughout the experiments. Their chemical compositions are illustrated in Table 1.

Table 1. Chemical composition of API X60 and 316 L steels.

Elements in wt%	C	Mn	Si	S	P	Cr	Mo	Ni
API X60	0.57-0.65	0.4-0.7	0.15-0.35	0.035	0.035	/	/	/
316L	≤ 0.03	≤ 2	≤ 1	≤ 0.01	≤ 0.04	16.5-18.5	2-2.5	10-13

The garlic material was obtained from a bulbous root of a local (Algerian) species. The freshly harvested plant was kept in the shade, in a dry and ventilated place. The garlic cloves were dried in the oven, at a temperature of 45 °C. After that, they were ground to obtain the garlic powder, of which 20 g were added to 100 mL of a hydro alcoholic mixture (30 mL of methanol + 70 mL of distilled water) [22].

In order to optimize flavour transfer, the mixture was subjected to continuous agitation, using a magnetic stirrer, at a temperature of 45 °C, until the garlic powder was completely impregnated in it (approx. 2 h), and then left at room temperature, for 24 h, to allow the isolation of the maximum active products, and to preserve their possible synergy. The obtained liquid (solute) was filtered, to remove the insoluble residues.

An evaporation phase, by means of a slight heating, was performed, to totally or partially remove the solvent. The obtained form, of which active principles are very concentrated, was stored at 4 °C. The unimolar H₂SO₄ was prepared by dilution of an analytical grade of H₂SO₄ (98%) with distilled water, and used as the corrosive test environment.

All experiments have been carried out without and with 20, 50, 100, 150 and 200 mg L⁻¹ of GE concentrations. The solution tests were prepared before each experiment.

PPD

PPD measurements were carried out at approx. 24 °C ambient temperature, in a conventional three-electrode cell. A saturated calomel electrode (SCE) and platinum electrode were used as reference and auxiliary electrodes, respectively. The working electrode (WE) was a conductor wire soldered with a steel coupon of 0.32 cm².

The isolation was obtained with an epoxy resin. Before each measurement, the surfaces were mechanically polished under water, with emery papers from 400 to 1200 mesh, then degreased in acetone, and rinsed with distilled water. Experiments were conducted by a Voltalab Radiometer Analytical set based on a PGZ 301 potentiostat, and controlled by Volta Master 4 acquisition software.

The PPD was carried out in the cathodic-anodic direction, from -0.25 to 2 V/E_{corr} (corrosion potential), at the scan rate of 1 mV s⁻¹, after a stabilization period of the abandoning potential (30 min). Corrosion current densities (i_{corr}) were obtained from the PPD curves by linear extrapolation of the Tafel curves. The IE% was calculated using the i_{corr} values, according to the following equation:

$$IE(\%) = \left(\frac{i_{corr}^* - i_{corr}}{i_{corr}^*} \right) \times 100 \quad (1)$$

where i_{corr} and i*_{corr} are the corrosion rates with and without GE, respectively.

EIS

EIS has been performed with the same equipment used for the linear polarization. Measurements were made around the equilibrium potential, using a sinusoidal signal, with an amplitude of 10 mV. The frequency was varied from 100 kHz to 10 mHz. The impedance diagrams are given in the Nyquist and Bode representations. Experiments were repeated three times, to ensure the reproducibility.

Results and discussion

316L SS PPD

Fig. 1 shows the cathodic and anodic polarization curves obtained for SS in a 1 M H₂SO₄ solution with and without GE.

PPD curves show that the solution with different GE concentrations displayed a decrease in the anodic and cathodic current densities (CD), and an E_{corr} towards more anodic values (> 85 mV) than those of uninhibited H₂SO₄, which reveals that the extract primarily acted as an anodic inhibitor [23, 24].

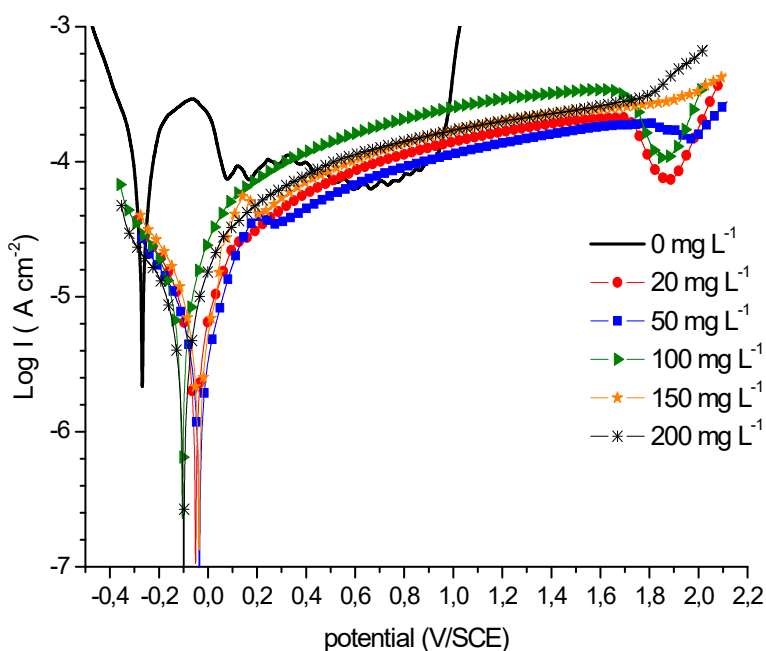


Figure 1. PPD curves for 316L SS in 1 M H₂SO₄ with different GE concentrations.

The cathodic curves are characterized by straight lines, according to Tafel linear law, whatever the GE concentration in the solution, which confirms that the inhibitor did not modify the proton discharge mechanism. The anodic branches of the PPD curves show the active-passive and passive-transpassive transitions in the uninhibited solution. In inhibited H₂SO₄, the current did not decrease, but there was a window of potential within which it slightly increased, displaying a pseudo-passive behaviour. According to Gonzalo et al. [25], this is obtained when the system is only partially passivated, or when the protective layer does not cover the entire surface. Indeed, the anodic PPD curves shape is strong related to the formation kinetics of the protective layer. Compared with the

anodic curve obtained without inhibitor, the transpassivation corresponding to a sharp increase in the current is obtained at much higher potentials, which indicates that the passive layer is more resistant. From such behaviour, it is difficult to unambiguously define the critical current (i_{cc}) and passivation potential (E_{pp}) values. The electrochemical parameters obtained from PPD curves, such as SS i_{corr} , E_{corr} and rupture potential (E_{rup}), as well as the GE IE%, at different concentrations, are given in Table 2.

Table 2. Electrochemical parameters for 316L SS in 1 M H₂SO₄, without and with GE, at different concentrations.

GE concentration (mg L ⁻¹)	i_{corr} (μ A/cm ²)	E_{rup} (V)	E_{corr} (mV)	IE (%)
-	91.51	0,98	-263	-
20	3.72	2.01	-47	95,93
50	2.08	2,15	-28	97.72
100	5.60	1.95	-98	93.88
150	2.90	1,95	-29	96.83
200	3.69	1.85	-92	95.96

These parameters reveal a significant difference in SS corrosion rate (CR) values in H₂SO₄ with and without inhibitor. In the solution without GE, the CD was about 91.5 μ A/cm². CDs decreased in H₂SO₄ with GE, at different concentrations, particularly when they were equal to 50 mg/L⁻¹. As a result, the IE was significantly increased, reaching a maximum value of 97.72%, at that concentration. GE corrosion inhibition compounds tend to slow down the charge transfer reaction (CTR) through interaction with the steel surface, and/or adsorption onto it.

To explain the inhibition mechanism, we have adopted one of two approaches: (1) the chemical (chemisorption) or physical (physisorption) approach that results from the interaction of the inhibitor polar centres with the metal active sites, which leads to the organic molecules adsorption onto the steel surface, with the formation of a protective layer; and (2) the formation of metal complexes when the inhibitors molecules react with the potential corrosion products in the media. Theoretical calculations in a previous study by Rodriguez-Clemente et al. [26], on CS inhibition by allicin, showed the formation of donor-accepter surface complexes between π -electrons, O and S atoms of the inhibitor molecules and the Fe unoccupied orbital ($[Fe-Inh]_{ads}^{2+}$). The adsorption of these complexes usually involves the replacement of water molecules absorbed onto the metal surface. As the concentration of the inhibitor increases, a compact complex with the metal ions is formed, so that the resulting adsorbed intermediate will be unready soluble in the acidic medium, which subsequently protects the metal from oxidation. With an increase in the inhibitor concentration greater than 50 mg/L⁻¹, more inhibitor molecules are available on the metal surface, and the $[Fe-Inh]^{2+}$ complex is desorbed from it, which removes its protection [26, 27].

XC60 CS linear polarization

When examining the overall PPD curves shown by Fig. 2, one notes that the GE addition, at different concentrations, to the 1 M H₂SO₄ solution, has not, in

general, a significant effect on the overall curves shape, as only a slight increase in the passivation potential occurs. The electrochemical parameters deduced from these curves are represented in Table 3.

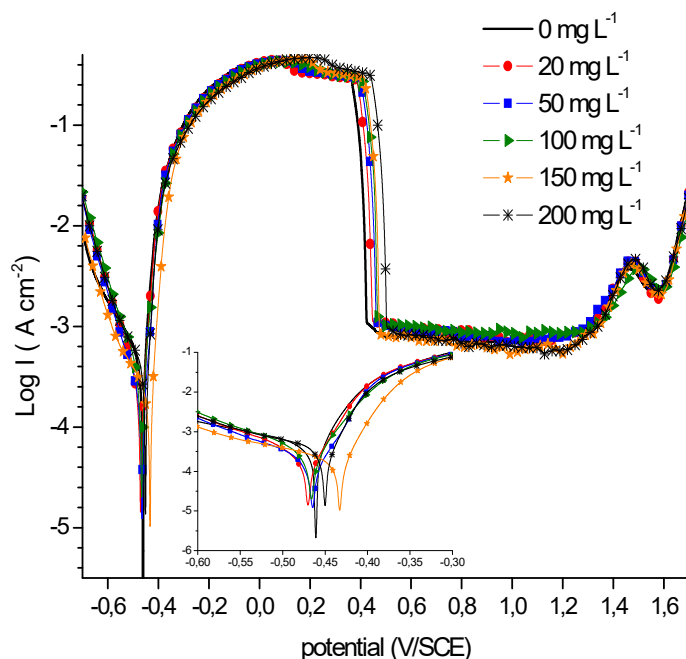


Figure 2. PPD curves for API X60 CS in 1 M H₂SO₄, at various GE concentrations.

Table 3. Electrochemical parameters for API X60 CS in 1 M H₂SO₄, at different GE concentrations.

GE concentration (mg L ⁻¹)	<i>i</i> _{corr} (μA/cm ²)	<i>E</i> _{rup} (V/SCE)	<i>E</i> _{corr} (mV/SCE)	IE (%)
-	418.9	1.62	-452.0	-
20	141.5	1.65	-461.5	66.22
50	136.4	1.65	-457.0	67.43
100	195.3	1.66	-458.0	53.37
150	121.4	1.64	-422.0	71.01
200	210.2	1.64	-439.0	49.82

The *E*_{corr} slightly fluctuated between lower and higher values, for higher and lower GE concentrations, respectively, without exceeding 85 mV, which suggests that it acted as a cathodic and anodic inhibitor [23, 24].

It can be seen, from PPD curves in Fig. 2, that the passivation stage kept practically the same passivation current value (*i*_{pass}) and *E*_{rup}. Moreover, with GE, the CS *i*_{corr} gradually decreased from 418.9 mA/cm² to 121.4 mA/cm², at the inhibitor concentration of 150 mg/L⁻¹, at which its CR was substantially lowered, thus giving the highest IE of 71.01% (Table 3).

The IEs were found to decrease as GE concentrations were increased from 49.82% to 71.01%. This behaviour can suggest a probable desorption of the GE layer from the CS surface. It is not easy to explain this behaviour, since the inhibitor effect and layer stability are directly related to its middle constitution, as well as to its acting mechanisms. Generally, the inhibition mechanism can be a

competition between chemisorption onto the metal and a combination between inhibitor ions and the metallic surface [28, 29]. As it was previously mentioned, the adsorbed inhibitor molecule (Inh_{ads}) may then combine with generated Fe^{2+} ions to form metal-inhibitor ($[\text{Fe-Inh}]_{\text{ads}}^{2+}$) complexes on the steel surface.

EIS measurements for 316L SS

Fig. 3 shows Nyquist impedance diagrams plotted at open circuit potential, for 316L SS in 1 M H_2SO_4 with different GE concentrations. Impedance diagrams show a series of capacitive loops, indicating that CTR controlled SS corrosion. The semicircle shape did not change with GE addition, which means that the corrosion mechanism has not changed [26].

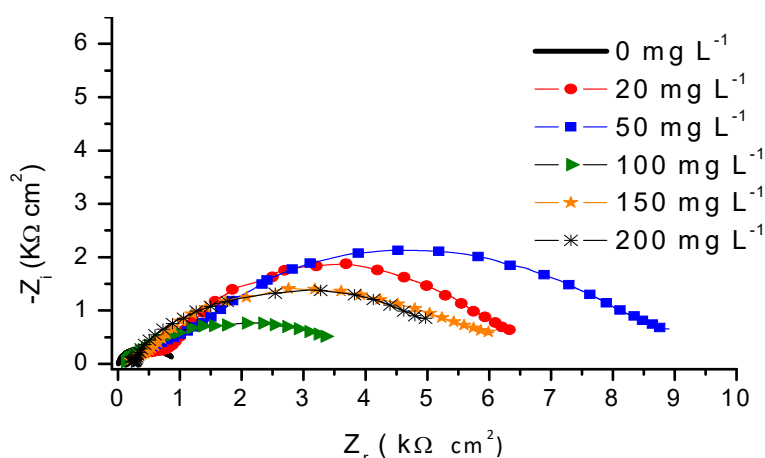


Figure 3. Nyquist plots of 316L SS in 1 M H_2SO_4 with different GE concentrations.

In fact, GE enhanced the charge transfer resistance (R_{tc}) value in H_2SO_4 . The capacitive loop diameter was larger than that of the uninhibited solution, and reached its maximum size with 50 mg L^{-1} of GE, starting to decrease at higher inhibitor concentrations.

The bode magnitude plots (Fig. 4-a) show that SS total impedance magnitudes at the lowest frequencies increased with GE, which indicates a higher CRST, due to the formation of a protective film. From the respective bode phase angle plots (Fig. 4-b), one can distinguish two peaks maxima that confirm the presence of two overlapping capacitive loops, in the Nyquist plots for SS treated with GE. The peak at high frequencies is due to the organic layer formed on the metal surface [30, 31], which results from the precipitation of various species naturally present in GE, such as S, amino acids and other organic compounds. The peak corresponding to the low frequency range is attributed to the oxide film formed due to the CTR on SS.

The Nyquist plot was expected to be a semicircle with its centre on the x-axis. However, the observed plots represent circle arcs with their centre located below the x-axis. These depressed semicircles can be explained by the heterogeneous nature of the SS surface or by the dispersion of some physical properties values of the system [31-33]. Consequently, the layer at the interface cannot be considered as an ideal capacitor, and the constant phase element (CPE) is often

used as a substitute for the latter. Therefore, the relevant impedance (Z_{CPE}) is defined as:

$$Z_{CPE} = \frac{1}{Q(j\omega)^n} \quad (2)$$

where Q is the CPE constant ($\Omega^{-1}/\text{cm}^{-2} \text{s}^n$). For $n = 1$, the CPE can be identified as the capacitance, and n is its exponent, such that $1 \geq n \geq 0$.

Since $n < 1$, the capacitance can be calculated from the CPE parameters, and R_{ct} is experimentally determined using the following equation [34]:

$$C = \frac{(QR_{ct})^{\frac{1}{n}}}{R_{ct}} \quad (3)$$

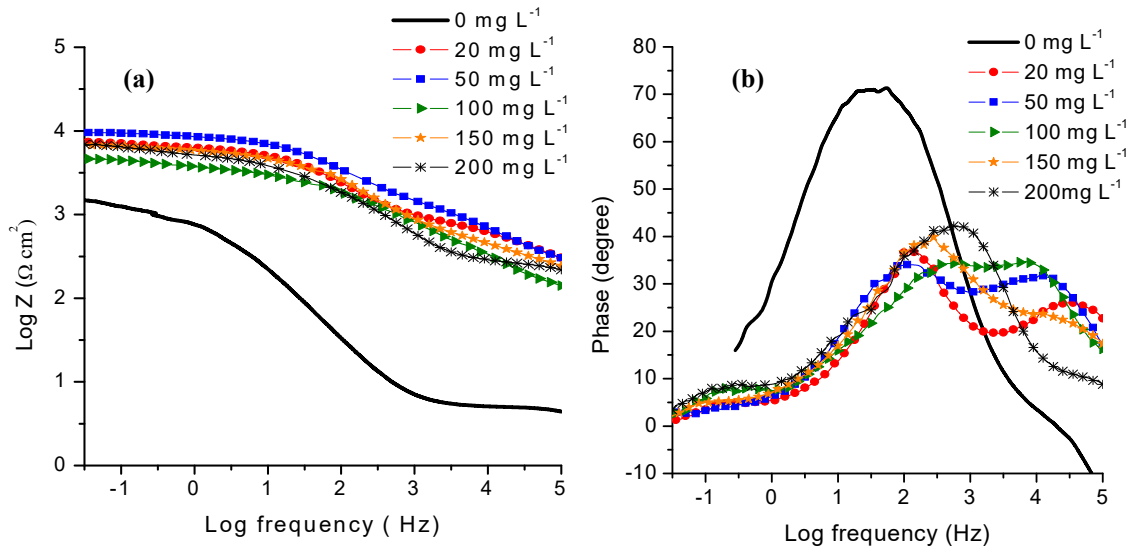


Figure 4. (a) Bode magnitude plots and (b) Bode phase angle plots of 316L SS in 1 M H₂SO₄ for different concentrations of GE.

The electrical circuit used to describe 316L SS exposed to H₂SO₄ with GE, taking account of the contribution of each phenomenon, such as CTR and protective film formation, is represented in Fig. 5.

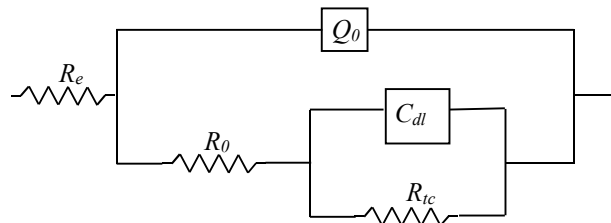


Figure 5. Equivalent circuit diagram for 316L SS exposed to H₂SO₄ with various GE concentrations.

where R_e is the electrolyte solution resistance, R_{ct} is the resistance associated with the CTR between the metal and the acidic medium, and C_{dl} is the non-ideal double layer capacitance, used in order to consider the interface roughness. R_0

and Q_0 are the parameters used when a protective inhibitor film is formed at the metal/solution interface.

The IE obtained from the R_{tc} is calculated by:

$$IE\% = \left(1 - \frac{R_{tc}^*}{R_{tc}}\right) \times 100 \quad (4)$$

where R_{tc}^* and R_{tc} are the transfer resistances with and without inhibitor, respectively. Impedance parameters obtained using the Z-view software are summarized in Table 4.

Table 4. Fitting parameters of impedance spectra for 316L SS exposed to H_2SO_4 with and without GE.

Concentration (mg L ⁻¹)	R_e (Ω cm ⁻²)	C_{dl} (Ω^{-1} cm ² s ⁿ).10 ⁵	n	R_{tc} (Ω cm ⁻²)	C_{eq} (μ F m ⁻²)	R_o (Ω cm ⁻²)	C_o (nFcm ⁻²)	IE (%)
blank	4.87	15.8	0.88	826.4	119	/	/	/
20	199.8	0.56	0.71	5813	1.38	858.7	28.83	85.77
50	155.3	0.56	0.63	8453	0.93	1529	26.31	90.22
100	108.2	1.68	0.51	3967	1.12	684.9	29.29	79.16
150	204.9	0.66	0.64	5763	1.05	1197	16.5	85.65
200	216.2	0.80	0.63	5227	1.24	994.8	31.66	84.18

The inhibited 316L SS sample shows higher R_{tc} values (8453 Ω cm⁻², at 50 mg/L⁻¹ GE) than the uninhibited one (826.4 Ω /cm⁻²). The above results may indicate that the inhibitor modified the 316L SS passive oxide film properties. The inhibited metal seems to have a quite high CRST, and, consequently, it obtains better corrosion protection (a probably more thick and compact layer) than the uninhibited one [35].

The surface inhomogeneity coefficient (n) values decrease with higher GE concentrations, due to the inhibitor molecules adsorption onto the SS surface. Moreover, the capacitance value (C_{eq}) obtained for the inhibited sample (≈ 1 μ F/cm⁻²) is lower than that for the uninhibited one (119 μ F/cm⁻²). Generally, the decrease in C_{eq} may be related to the growing metal surface thickness due to the formation of a protective layer created by the inhibitor compounds adsorption onto SS [35, 36]. Also, the replacement of the adsorbed water molecules, at the surface metal, by the inhibitor, which has a lower dielectric constant, may be considered as another reason for the C_{eq} decrease [37].

EIS measurements for API X60 CS

Figs. 6 and 7 show Nyquist impedance and Bode diagrams of API X60 CS in 1 M H_2SO_4 with GE, at different concentrations. As observed in Nyquist diagrams, one great capacitive semicircle can be observed over the whole frequency range.

As illustrated by Fig. 7a, at a low frequency region, magnitude values corresponding to the R_{tc} increase, with GE. Consequently, GE has a beneficial influence on the CS CRST.

The phase angle presents only one peak maximum (between 10² and 10³ Hz), which leads to the use of a simple Randles circuit, for fitting the data, as shown by Fig. 8.

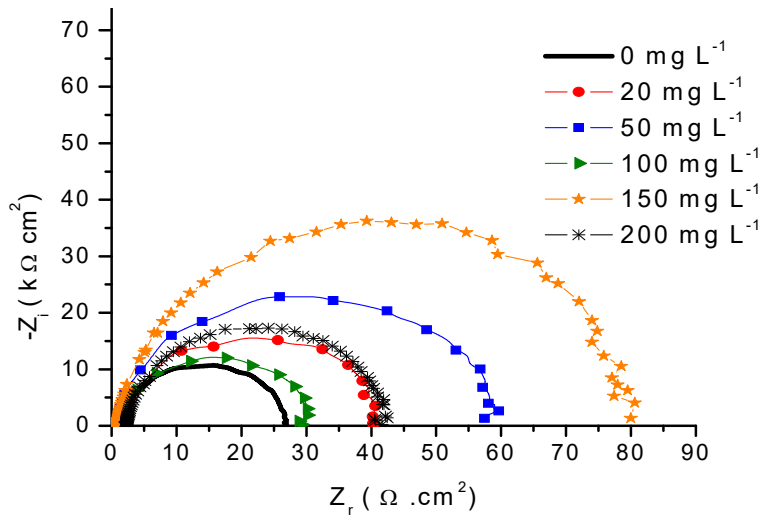


Figure 6. Nyquist plots of API X60 CS in 1 M H₂SO₄ at various GE concentrations.

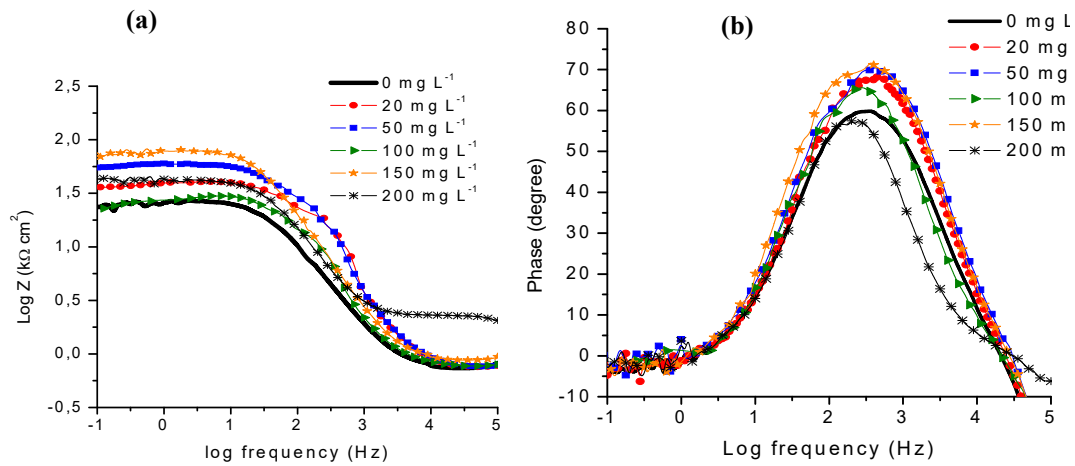


Figure 7. (a) Bode magnitude plots and **(b)** Bode phase angle plots of API X60 CS in 1 M H₂SO₄ at various GE concentrations.

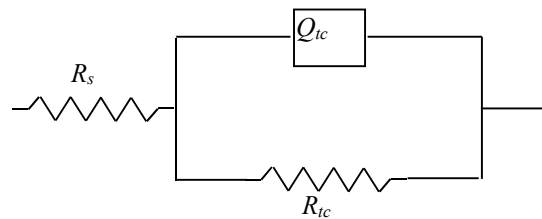


Figure 8. The equivalent circuit diagram for API X60 CS exposed to 1 M H₂SO₄ at various GE concentrations.

Table 5 summarizes the electrochemical parameters deduced from the impedance spectra, in addition to the IE determined by the relation (4). According to these results, it can be seen that the inhibitor increased the R_{tc} , which reached a maximum value of $77.08 \Omega/\text{cm}^2$, at 150 mg/L^{-1} GE. For this concentration, the IE was maximum, reaching 67.06%. The C_{eq} decreased when R_{tc} increased,

indicating a modification in the oxide film properties formed on the CS surface. This can be explained by the increase in the film thickness and/or compactness, which is related to the decrease in its permittivity. These results are in good agreement with those determined from the PPD curves.

Table 5. Fitting parameters of impedance spectra for API X60 CS exposed to H₂SO₄ with and without GE.

Concentration (mg L ⁻¹)	R_e (Ω cm ⁻²)	C_{dl} (Ω^{-1} cm ⁻² s ⁿ).10 ⁵	n	R_{tc} (Ω cm ⁻²)	C_{eq} (μ F m ⁻²)	IE (%)
-	0.76	27	0.89	25.39	146.2	-
20	0.77	14	0.93	39.93	94.8	36.41
50	0.78	12	0.94	57.49	87.5	54.89
100	0.78	23	0.93	29.92	158	15.14
150	0.91	10	0.94	77.08	73.5	67.06
200	2.24	16	0.93	39.99	109.5	36.50

Conclusions

The GE effect on API X60 CS and 316L SS corrosion, in a 1 M H₂SO₄ solution, was studied. A comparative analysis was carried out on the inhibited and uninhibited samples, using two electrochemical techniques. The results obtained from the PDP show that GE inhibited both anodic metal dissolution and cathodic hydrogen evolution, and corroborate the EIS results. It was shown that this inhibitor decreased CR and increased charge transfer and polarization resistances for both metals, as time elapsed until a certain period, after which the protective film started to desorb from the steel surfaces.

Complex impedance plots exhibited one and two deformed capacitating semi-circles for API X60 CS and 316L SS, respectively. In the first case, a circuit with a single time constant represented the interface. However, an equivalent circuit with two time constants indicated that the protective film (organic compounds) recovered the metal, in addition to the CTR occurring on the SS/solution interface.

The IE increased significantly, exceeding 90% and 65%, for 316L SS and API X60 CS corrosion, respectively. This favourable behaviour can be related to the protective layer formed by several organic compounds existing in the garlic, which work as a barrier between the steels and H₂SO₄. Consequently, GE mainly acts as a good corrosion inhibitor for the studied steels and, eventually, as a promising green inhibitor for others systems. More investigations are still needed, to determine whether the action of the compounds is synergetic, or just the superimposition of the individual effect.

Authors' contributions

S. Belkaid: conceived the research idea and supervised the work; designed and performed the experiments; performed the equivalent circuit diagrams for parameters calculations; wrote the manuscript in consultation with all authors. **S. Hamdani:** verified the numerical results; contributed to the paper writing. **D. Mansour:** manufactured samples and prepared solutions and GE; contributed to the paper writing.

References

1. Yaro AS, Khadom AA, Wael RK. Apricot juice as green corrosion inhibitor of mild steel in phosphoric acid. *Alexandria Eng J.* 2013;52:129-135. DOI: <https://doi.org/10.1016/j.aej.2012.11.001>
2. Al-Otaibi MS, Al-Mayouf AM, Khan M, et al. Corrosion inhibitory action of some plant extracts on the corrosion of mild steel in acidic media. *Arabian J Chem.* 2014;7:340-346. DOI: <https://doi.org/10.1016/j.arabjc.2012.01.015>
3. Abdel-Gaber M, Abd-El-Nabey BA, Sidahmed IM, et al. Inhibitive action of some plant extracts on the corrosion of steel in acid media. *Corr Sci.* 2006;48:2765-2779. DOI: <https://doi.org/10.1016/j.corsci.2005.09.017>
4. Khadom AA, Yaro AS, Altaie AS, et al. Electrochemical activations and adsorption studies for the corrosion inhibition of low carbon steel in acidic media. *Port Electrochim Acta.* 2009;27:699-712. DOI: <https://doi.org/10.4152/pea.200906699>
5. Musa AY, Khadom AA, Kadhum AAH, et al. Kinetic behavior of mild steel corrosion inhibition by 4-amino-5-phenyl-4H-1,2,4-triazole-3-thiol. *J Taiwan Inst Chem Eng.* 2010;41:126-128. DOI: <https://doi.org/10.1016/j.jtice.2009.08.002>
6. Arockia Selvi J, Rajendran S, Ganga Sri V, et al. Corrosion inhibition by Beet Root extract. *Port Electrochim Acta.* 2009;27:1-11. DOI: <https://doi.org/10.4152/pea.200901001>
7. Riggs OL. *Corrosion Inhibitors.* C.C. Nathan. 2nd Ed. NACE; 1973.
8. Benmessaoud Left D, Zertoubi M, Irhzo A, et al. Oils and extracts plants as corrosion inhibitors for different metals and alloys in hydrochloric acid medium. *J Mat and Environ Sci.* 2013;4:855-866.
9. Nazir I, Chauhan R. Qualitative phytochemical analysis of *Allium sativum* (Garlic) and *Curcuma longa* (Turmeric). *J Entom and Zool Stud.* 2019;7:545-547.
10. Loto RT, Loto CA, Joseph O, et al. Adsorption and corrosion inhibition properties of thiocarbanilide on the electrochemical behavior of high carbon steel in dilute acid solutions. *Results in Physics.* 2016;6:305-314. DOI: <https://doi.org/10.1016/j.rinp.2016.05.013>
11. Ferreira ES, Giacomelli C, Giacomelli FC, et al. Evaluation of the inhibitor effect of L-ascorbic acid on the corrosion of mild steel. *Mat Chem and Phys.* 2004; 83:129-134. DOI: <https://doi.org/10.1016/j.matchemphys.2003.09.020>
12. Yildirim A, Cetin M. Synthesis and evaluation of new long alkyl side chain acetamide, isoxazolidine and isoxazoline derivatives as corrosion inhibitors. *Corr Sci.* 2008;50:155-165. DOI: <https://doi.org/10.1016/j.corsci.2007.06.015>
13. Saedah Al-Mhyawi R. Corrosion inhibition of aluminum in 0.5 m HCl by garlic aqueous extract. *Orient J Chem.* 2014;30:541-552. DOI: <http://dx.doi.org/10.13005/ojc/300218>
14. Ali M, Ibrahim I. Phytochemical screening and proximate analysis of Garlic (*Allium Sativum*). *Arch of Organ and Inorgan Chem Sci.* 2019;4:478-482. DOI: <https://doi.org/10.32474/AOICS.2019.04.000180>
15. Block E. The chemistry of garlic and onions. *Scientific American.* 1985;252:114-119. DOI: <https://doi.org/10.1038/scientificamerican0385-114>
16. Nakamoto M, Kunimura K, Suzuki JI, et al. Antimicrobial properties of hydrophobic compounds in garlic: Allicin, vinylidithiin, ajoene and diallyl

- polysulfides (Review). *Experim and Therap Med.* 2020;19(2):1550-1553. DOI: <https://doi.org/doi.org/10.3892/etm.2019.8388>
17. Getti GTM, Poole PL. Allicin causes fragmentation of the peptidoglycan coat in *Staphylococcus aureus* by effecting synthesis and aiding hydrolysis: A determination by MALDI-TOF mass spectrometry on whole cells. *J Med and Microb.* 2019;68:667-677. DOI: <https://doi.org/10.1099/jmm.0.000950>
 18. Wang HP, Yang J, Qin LQ. Effect of Garlic on Blood Pressure: A Meta-Analysis. *J Clin Hypertens.* 2015;17(3). DOI: <https://doi.org/10.1111/jch.12473>
 19. Aniekan I, Ejiroghene O, Abdulsamad G. Engineering material selection for automotive exhaust systems using CES software. *Int J Eng Technol.* 2017;3:50-60. DOI: <https://doi.org/10.19072/ijet.282847>
 20. Lakshmi PS, Chitra A, Rajendran S, et al. Corrosion behavior of aluminum in rain water containing GE. *Surf Eng.* 2005;21(3):229-231. DOI: <https://doi.org/10.1179/174329405X50073>
 19. Barreto LS, Tokumoto MS, Guedes IC, et al. Evaluation of the anticorrosion performance of peel GE as corrosion inhibitor for ASTM 1020 carbon steel in acidic solution. *Matéria.* 2017;22(3). DOI: <https://doi.org/10.1590/S1517-707620170003.0186>
 20. Taha AA, Abouzeid FM, Elsadek MM, et al. Effect of methanolic plant extract on copper electro-polishing in ortho-phosphoric acid. *Arabian J Chem.* 2020;13(8):6606-6625. DOI: <https://doi.org/10.1016/j.arabjc.2020.06.017>
 23. Luo X, Pan X, Yuan S, et al. Corrosion inhibition of mild steel in simulated seawater solution by a green eco-friendly mixture of glucomannan (GL) and bisquaternary ammonium salt (BQAS). *Corros Sci.* 2015;125:139-151. DOI: <https://doi.org/10.1016/j.corsci.2017.06.013>
 24. Idouhli R, Koumya Y, Khadiri M, et al. Inhibitory effect of *Senecio anteuphorbium* as green corrosion inhibitor for S300 steel. *Int J Industr Chem.* 2019;10:133-143. DOI: <https://doi.org/10.1007/s40090-019-0179-2>
 25. Gonzalo V, Berny RV, David GD. The active-passive behavior of chalcopyrite comparative study between electrochemical and leaching responses. *J Electrochem Soc.* 2007;154:299-311. DOI: <https://doi.org/10.1149/1.2721782>
 26. Rodriguez-Clemente E, Gonzalez-Rodriguez JG, Valladarez-Cisneros MG, et al. Experimental and Theoretical Evaluation of Allicin as Corrosion Inhibitor for carbon steel in Sulfuric Acid. *J Mat and Environ Sci.* 2017;8(11):3817-3833.
 27. Ahamad I, Quraishi MA. Mebendazole: New and efficient corrosion inhibitor for mild steel in acid medium. *Corr Sci.* 2010;52:651-656. DOI: <https://doi.org/10.1016/j.corsci.2009.10.012>
 28. Hong J, Zhen-Peng K, Yan L. Aminic nitrogen-bearing polydentate Schiff base compounds as corrosion inhibitors for iron in acidic media: A quantum chemical calculation. *Corros Sci.* 2008;50:865-871. DOI: <https://doi.org/10.1016/j.corsci.2007.10.009>
 29. Hukovic-Metikos M, Babić R, Grubač Z. Study of aluminium corrosion in acidic solution with nontoxic inhibitors. *J Appl Electrochem.* 2002;32:35-41. DOI: <https://doi.org/10.1023/A:1014265407060>

30. Traisne IBF, Lagrenee M. The substituted 1,3,4-oxadiazoles: a new class of corrosion inhibitors of mild steel in acidic media. *Corros Sci.* 2000;42:127-146. DOI: [https://doi.org/10.1016/S0010-938X\(99\)00049-9](https://doi.org/10.1016/S0010-938X(99)00049-9)
31. Yuan SJ, Choong AMF, Pehkonen SO. The influence of the marine aerobic *Pseudomonas* strain on the corrosion of 70/30 Cu–Ni alloy. *Corros Sci.* 2007;49:4352-4385. DOI: <https://doi.org/10.1016/j.corsci.2007.04.009>
32. Xu X, Ma H, Chen S, et al. General equivalent circuits for faradaic electrode processes under electrochemical reaction control. *J Electrochem Soc.* 1999;146:847-854. DOI: <https://doi.org/10.1149/1.1391854>
33. Belkaid S, Hamdani S, Ladjouzi MA. Effect of biofilm on naval steel corrosion in natural seawater. *J Solid State Electrochem.* 2010;15:525-537. DOI: <https://doi.org/10.1007/s10008-010-1118-5>
34. Bouckamp BA. Users Man Equivalent circuit.ver 4.51, Faculty of chemical Technology, University of Twente, The Netherlands. 1993.
35. Bammou L, Belkhaouda M, Salghi R, et al. Corrosion inhibition of steel in sulphuric acidic solution by the *Chenopodium Ambrosioides* Extracts. *J Associat Arab Univ Basic Appl Sci.* 2014;16:83-90. DOI: <https://doi.org/10.1016/j.jaubas.2013.11.001>
36. Lebrini M, Lagrenee M, Vezin H, et al. Experimental and theoretical study for corrosion inhibition of mild steel in normal hydrochloric acid solution by some new macrocyclic polyether compounds. *Corr Sci.* 2007;49:2254-2269. DOI: <https://doi.org/10.1016/j.corsci.2006.10.029>
37. Solmaz R, Kardas G, Culha M, et al. Investigation of adsorption and inhibitive effect of 2-mercaptothiazoline on corrosion of mild steel in hydrochloric acid media. *Electrochim Acta.* 2008;53:5941-5952. DOI: <https://doi.org/10.1016/j.electacta.2008.03.055>